ACCOUNTS
of chemical research

Artificial Metalloenzymes Based on the Biotin–Avidin Technology: Enantioselective Catalysis and Beyond

THOMAS R. WARD*
Department of Chemistry, University of Basel, Spitalstrasse 51, CH-4056 Basel, Switzerland

RECEIVED ON JULY 10, 2010

CONSPECTUS

Artificial metalloenzymes are created by incorporating an organometallic catalyst within a host protein. The resulting hybrid can thus provide access to the best features of two distinct, and often complementary, systems: homogeneous and enzymatic catalysts. The coenzyme may be positioned with covalent, dative, or supramolecular anchoring strategies. Although initial reports date to the late 1970s, artificial metalloenzymes for enantioselective catalysis have gained significant momentum only in the past decade, with the aim of complementing homogeneous, enzymatic, heterogeneous, and organic catalysts.

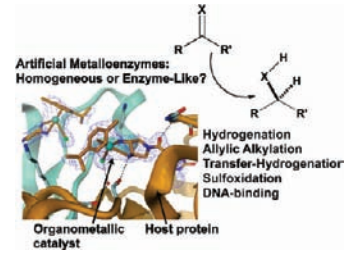

Inspired by a visionary report by Wilson and Whitesides in 1978, we have exploited the potential of biotin–avidin technology in creating artificial metalloenzymes. Owing to the remarkable affinity of biotin for either avidin or streptavidin, covalent linking of a biotin anchor to a catalyst precursor ensures that, upon stoichiometric addition of (strept)avidin, the metal moiety is quantitatively incorporated within the host protein. In this Account, we review our progress in preparing and optimizing these artificial metalloenzymes, beginning with catalytic hydrogenation as a model and expanding from there.

These artificial metalloenzymes can be optimized by both chemical (variation of the biotin–spacer–ligand moiety) and genetic (mutation of avidin or streptavidin) means. Such chemogenetic optimization schemes were applied to various enantioselective transformations. The reactions implemented thus far include the following: (i) The rhodium-diphosphine catalyzed hydrogenation of *N*-protected dehydroaminoacids (ee up to 95%); (ii) the palladium-diphosphine catalyzed allylic alkylation of 1,3-diphenylallylacetate (ee up to 95%); (iii) the ruthenium pianostool-catalyzed transfer hydrogenation of prochiral ketones (ee up to 97% for aryl-alkyl ketones and ee up to 90% for dialkyl ketones); (iv) the vanadyl-catalyzed oxidation of prochiral sulfides (ee up to 93%).

A number of noteworthy features are reminiscent of homogeneous catalysis, including straightforward access to both enantiomers of the product, the broad substrate scope, organic solvent tolerance, and an accessible range of reactions that are typical of homogeneous catalysts. Enzyme-like features include access to genetic optimization, an aqueous medium as the preferred solvent, Michaelis–Menten behavior, and single-substrate derivatization. The X-ray characterization of artificial metalloenzymes provides fascinating insight into possible enantioselection mechanisms involving a well-defined second coordination sphere environment. Thus, such artificial metalloenzymes combine attractive features of both homogeneous and enzymatic kingdoms.

In the spirit of surface borrowing, that is, modulating ligand affinity by harnessing existing protein surfaces, this strategy can be extended to selectively binding streptavidin-incorporated biotinylated ruthenium pianostool complexes to telomeric DNA. This application paves the way for chemical biology applications of artificial metalloenzymes.

Introduction

Traditionally, catalysis has been classified in three distinct categories: heterogeneous, homogeneous, and enzymatic catalysis. For the synthesis of high-added value chemicals, both homogeneous and enzymatic catalysis have found widespread use.[1]

In many respects, homogeneous and enzymatic catalysis are complementary (Table 1).[2]

Published on the Web 10/15/2010 www.pubs.acs.org/acr
10.1021/ar100099u

TABLE 1. Summary of Features of Homogeneous and Enzymatic Catalysis

	homogeneous	enzymatic
enantiomers	easy access	challenging
solvent tolerance	mostly organic	mostly aqueous
substrate scope	large	narrow
optimization	chemical	genetic
turnover number	limited	large
metals involved	any metal	limited (biorelevant)

Whereas it is straightforward to generate both enantiomers of a product using homogeneous catalysis, inverting the enantioselectivity of an enzyme is challenging. Many enzymes evolved to target a single substrate or functionality. In contrast, the best homogeneous catalysts display a broad substrate scope. For optimization, parallel synthesis generates libraries of a few hundred ligands. Directed evolution generates tens of thousands of mutants. Given an efficient screening tool,[3] enzymes can be evolved to overcome most of their limitations listed in Table 1.

Inspection of homogeneous and enzymatic catalytic systems reveals differences in the second coordination sphere of Knowles' [Rh(dipamp)(olefin)]$^+$ compared to Cytochrome P450 with its camphor substrate bound (Figure 1). In the case of [Rh(dipamp)]$^+$, the enantiopure ligand which provides the first coordination sphere occupies one hemisphere around the metal while the prochiral olefinic substrate is bound to the opposite hemisphere. For 40 years, design in enantioselective catalysis focused on extending the reach of the enantiopure ligands to better control the enantiodiscrimination. In contrast, camphor is completely embedded within a protein environment (which provides a well ordered second coordination sphere), conferring exquisite levels of selectivity to Cytochrome P450. In addition, the first coordination sphere (i.e., ligands bound to the metal) around iron is achiral.

With the aim of complementing these well established fields, organocatalysis and artificial metalloenzymes have attracted attention in the past decade.[4] Artificial metalloenzymes result from incorporation of a metal-containing moiety within a protein scaffold, thus conferring novel catalytic function to the macromolecule.[5] To ensure localization of the artificial cofactor, three anchoring strategies have been pursued: covalent, dative, or supramolecular. Although initial reports were published in the late 1970s by Kaiser and coworkers[6] (covalent and dative) and Whitesides and Wilson[7] (supramolecular), the field remained unexplored for over 20 years.[8] Thereafter, several groups have reported on their efforts to create artificial metalloenzymes for enantioselective catalysis.[8d,9]

Our interest in the field was derived from attempts to generate catalytic antibodies bearing a dinuclear metal cofactor. Faced with the difficulty of covalently tethering a divanadyl-containing transition-state analogue to a carrier protein for immunization,[10] we sought alternative strategies to create artificial metalloenzymes. We reasoned that, rather than relying on the immune response to generate a protein, we could use recombinant technology to produce and subsequently optimize the host protein. In this context, we stumbled across Whitesides' visionary communication reporting on the use of [Rh(NBD)(**Biot-1**)]$^+\subset$Avidin for the enantioselective hydrogenation of *N*-acetamido acrylic acid (up to 41% ee).[7] ($\subset$ symbolizes the inclusion of an artificial cofactor within a host protein.) Although such a host protein was by no means optimized for enantioselective catalysis, we hypothesized that we could evolve artificial metalloenzymes by combining both chemical and genetic means (Figure 2).

Hydrogenation as Model Reaction

Our initial efforts aimed at reproducing Whitesides' results using commercially available avidin. Conjecturing that the high pI of avidin (pI: 10.4) may significantly reduce the affinity of cationic complexes [Rh(COD)(**biot-1**)]$^+$ for the host pro-

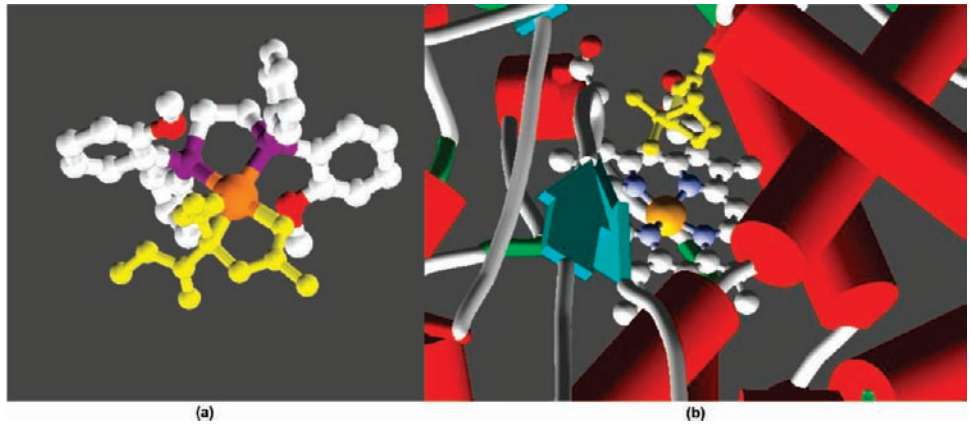

FIGURE 1. Structure of [Rh(dipamp)]$^+$ (CSD: VERYAS) (a) and Cytochrome P450 (PDB: 2CPP) (b) bound to their respective substrates (yellow).

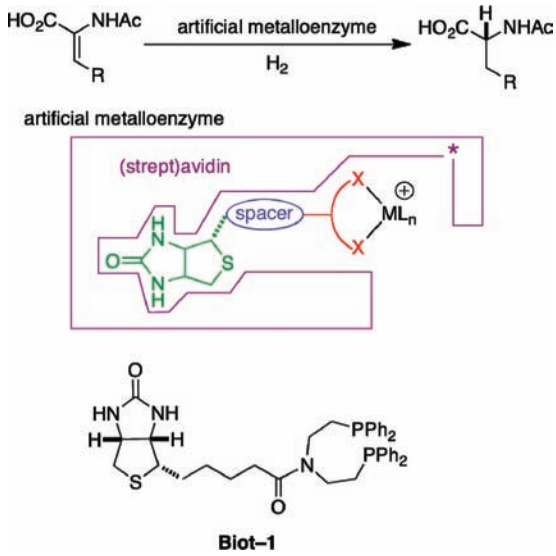

FIGURE 2. Artificial metalloenzymes based on the biotin−avidin technology. Whitesides' initial report (a). A chemogenetic optimization scheme allows one to improve the performance of the hybrid catalyst either by varying the spacer (oval) or the chelating ligand, or by mutating the gene of the host protein (*).

tein, we expressed streptavidin (Sav, pI: 6.2) in *E. coli*.[11] Both Avi and Sav are homotetrameric eight-stranded β-barrels (30% sequence identity, 42% sequence similarity) and bind with similar affinities to biotin ($K_a > 10^{13}$ M^{-1}). We were pleased to find that, under identical conditions, [Rh(COD)(**biot-1**)]$^+$⊂Sav afforded (*R*)-*N*-acetamidoalanine (*N*-AcAla) in 92% ee and quantitative conversion using 0.9 mol % Rh.[12]

Inspection of the docked complex [Rh(COD)(**biot-1**)]$^+$⊂Sav led us to identify position S112 as the closest lying residue to the rhodium (see Figure 7 for close lying amino acids).[13] For genetic optimization purposes, we expressed the 20 Sav isoforms resulting from saturation mutagenesis at position S112. These mutants were screened with a library of 18 biotinylated ligands, either differing in the chelating bisdiphenylphosphino moiety or in the spacer. A major screening campaign was undertaken: the 18 ligands were combined with the 20 Sav isoforms S112X, and the resulting artificial metalloenzymes were tested with both *N*-acetamidocinnamic acid and *N*-acetamidoacrylic acid to afford *N*-acetamidophenylalanine (*N*-AcPhe) and (*N*-AcAla) respectively (Figure 3).[14]

Subsequently, we included enantiopure aminoacid spacers between biotin and the ligand **1** to yield **biot-Phe-1** and **biot-Pro-1**.[16] A selection of results is presented in Table 2.

Several fascinating features emerge from this screening:

(i) The chemical optimization affords more diversity than the genetic optimization (compare lines with columns in Figure 3). While each spacer−ligand combination projects the metal moiety in a different chiral environment, genetic optimization can be regarded as fine-tuning of the second coordination sphere.

(ii) The flexible ligand scaffold **1** affords higher activities and selectivities than the six-membered ring chelate derived from ligand **2** (exception: Table 2 entry 6). This suggests that the ligand adopts an enantioenriched conformation upon docking in the protein. We view this phenomenon as an "induced lock-and-key" mechanism.

(iii) In most cases, the selectivities and conversions for both *N*-AcAla and *N*-AcPhe are comparable, reminiscent of the broad substrate scope observed with most homogeneous catalysts. However, certain ligand-protein combinations afford distinct differences for both substrates (Table 2, entry 5). Interestingly, a single point mutation allows to invert the enantioselectivity (Table 2, entries 13−14).

(iv) The highest (*S*)-selectivities using achiral spacers are obtained upon combining **biot-4*^{meta}*-1** with cationic residues at position S112 (Table 2, entries 2, 3).

(v) Incorporation of enantiopure spacers significantly improves the (*S*)-selectivity and affords promising hybrid catalysts with Avi (Table 2, entries 7−14). In addition, conformationally constrained spacers (**biot-(*R*)-Pro-1**) significantly improve the stability of the resulting artificial metalloenzyme toward organic solvents (Table 2, entries 9, 10).

(vi) Both the homogeneous catalyst [Rh(COD)(**biot-1**)]$^+$ (k_{cat} 3.06 min^{-1}; K_M 7.38 mM) and the artificial metalloenzyme [Rh(COD)(**biot-(*R*)-Pro-1**)]$^+$⊂Sav (k_{cat} 12.30 min^{-1}; K_M 4.36 mM) display Michaelis−Menten kinetics and a slight rate acceleration for the hybrid catalyst.

Following our publications, Reetz and co-workers reported on a directed evolution strategy to optimize artificial hydrogenases based on [Rh(COD)(**biot-1**)]$^+$⊂Sav and mutants thereof for the reduction of methyl-*N*-acetamidoacrylate. Faced with difficulties related to the need of purified proteins for screening purposes, they relied on focused libraries bearing mutations only at selected positions. The selectivities however remained modest (65% ee for (*R*)-Me-*N*-AcAla and −7% ee for (*S*)-Me-*N*-AcAla).[17]

Having demonstrated the potential of the chemogenetic optimization scheme for artificial hydrogenases, we focused on other enantioselective transformations. We selected reactions for which one of the substrates is not bound to the metal in the transition state (Figure 4). Upon incorporation of the artificial coenzyme within Sav, we anticipated that the second coordination sphere environment provided by the protein may steer the selective delivery of this substrate and thus influence the enantioselectivity.

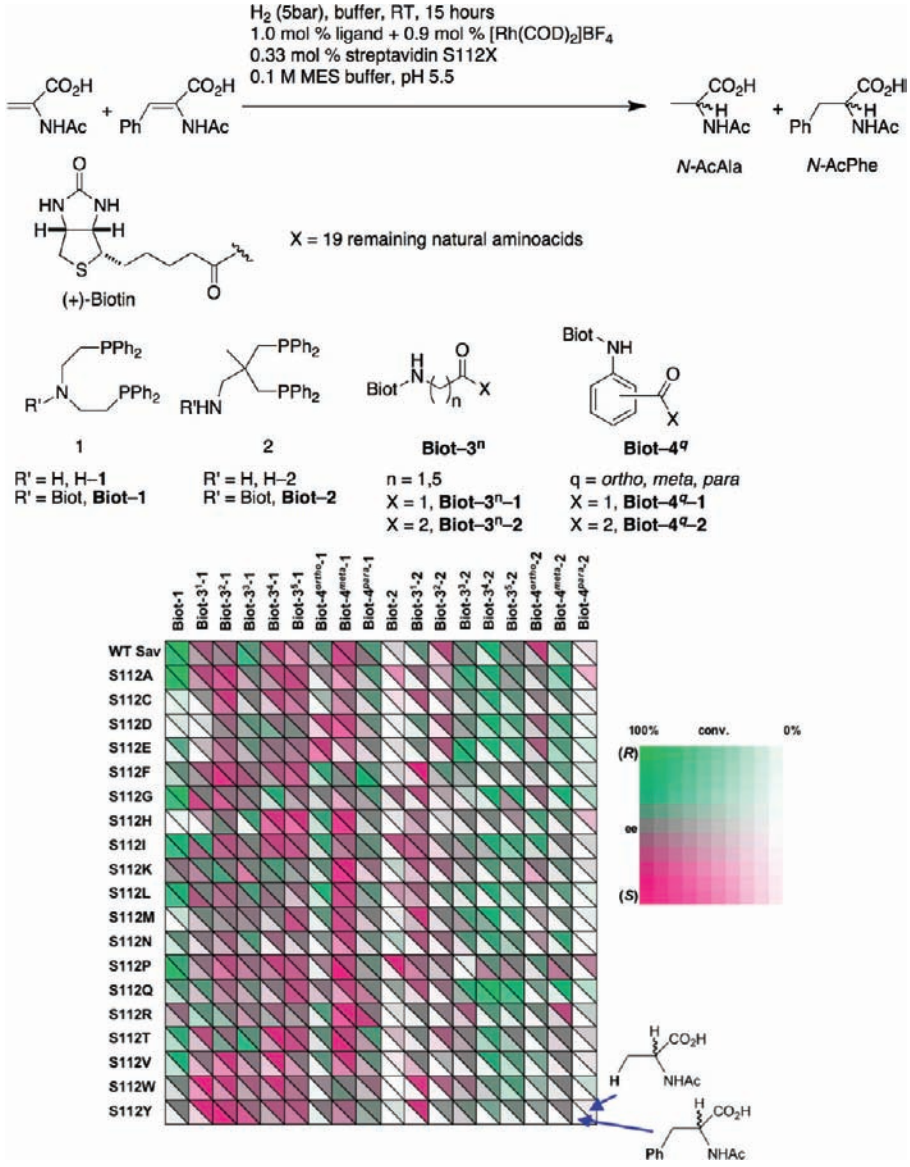

FIGURE 3. Operating conditions (top) and fingerprint display[15] of the results (bottom) for the chemogenetic optimization of artificial hydrogenases for the reduction of *N*-acetamidocinnamic acid and *N*-acetamidoacrylic acid. Adapted with permission from ref 14. Copyright 2005 Wiley VCH.

The Allylic Alkylation

The Asymmetric allylic alkylation (AAA) proceeds without prior coordination of the soft nucleophile to the palladium center.[18] Although many efficient homogeneous catalysts for the alkylation of 1,3-diphenylallylacetate rely an electronically asymmetric ligand,[19] we hypothesized that the library of ligands and proteins used for the artificial hydrogenases could be screened in the presence of a palladium precursor for the AAA. An initial screen of biotinylated imine and phosphine ligands (with no spacer) in the presence of Sav revealed that **biot-1** was the most promising scaffold. In most cases, neither alkylation product nor starting material could be detected: only the hydrolysis product (1,3-diphenylallylalcohol) was identified by HPLC. To circumvent this, addition of a surfactant (didodecyldimethylammonium bromide, DMB) suppressed the side reaction.

Having identified suitable reaction conditions, a library of 14 complexes [Pd(η^3-allyl)(**biot-spacer-1**)]$^+$ were screened with the saturation mutagenesis library S112X Sav as well as double mutants (Figure 5).[20]

Several noteworthy features were identified:

(i) Most artificial metalloenzymes were inactive in the AAA, yielding hydrolysis product. Notable exceptions incorporated **biot-3^1-1** (racemic product), **biot-4^{ortho}-1** (mostly (*R*) product, Table 3, entries 1–3 with an exception, entry 4), and **biot-(*R*)-Pro-1** ((*S*)-product, Table 3, entries 5, 6).

TABLE 2. Nummerical Summary of Selected Results for Artificial Hydrogenases

			N-AcPhe		*N*-AcAla[a]	
entry	ligand	protein	ee	conv.	ee	conv.
1	**biot-1**	WT Sav	93 (*R*)	84	94 (*R*)	quant.
2	**biot-4^{meta}-1**	S112H	81 (*S*)	88	58 (*S*)	quant.
3	**biot-4^{meta}-1**	S112K	88 (*S*)	89	63 (*S*)	quant.
4	**biot-4^{meta}-1**	S112R	86 (*S*)	71	63 (*S*)	quant.
5	**biot-3^{1}-2**	S112W	33 (*S*)	8	59 (*S*)	96
6	**biot-3^{4}-2**	S112Q	92 (*R*)	77	87 (*R*)	quant.
7	**biot-(*R*)-Pro-1**	WT Avi	89 (*S*)	quant.	87 (*S*)	quant.
8	**biot-(*R*)-Pro-1**	WT Sav	91 (*S*)	quant.	86 (*S*)	quant.
9	**biot-(*R*)-Pro-1**	WT Sav[b]	86 (*S*)	94	87 (*S*)	quant.
10	**biot-(*R*)-Pro-1**	WT Sav[c]	87 (*S*)	85	83 (*S*)	90
11	**biot-(*R*)-Pro-1**	WT Sav[d]	89 (*S*)	36	76 (*S*)	76
12	**biot-(*R*)-Pro-1**	S112W	95 (*S*)	quant.	95 (*S*)	quant.
13	**biot-(*S*)-Phe-1**	S112H	78 (*S*)	65	87 (*S*)	quant.
14	**biot-(*S*)-Phe-1**	S112M	87 (*R*)	quant.	73 (*R*)	quant.

[a] quant.: quantitative conversion. [b] Reaction carried out in 45% DMSO. [c] Biphasic with EtOAc. [d] Protein immobilized on biotin-sepharose.

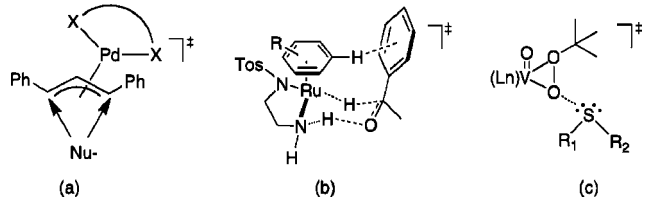

FIGURE 4. Postulated transition states for catalysts where one of the substrates does not bind to the metal: asymmetric allylic alkylation (a), asymmetric transfer hydrogenation (b), and sulfoxidation (c).

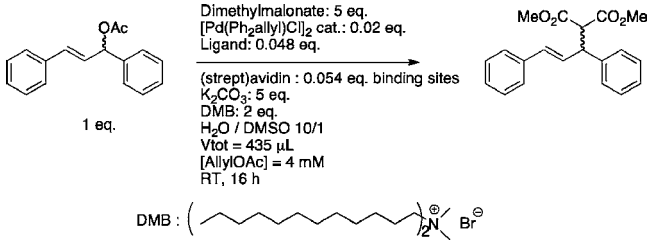

FIGURE 5. Operating conditions for the AAA catalyzed by artificial metalloenzymes based on the biotin−avidin technology (for ligands, see Figure 3).

TABLE 3. Numerical Summary of Selected AAA Results

entry	ligand	protein	ee (%)	conv. (%)
1	**biot-4^{ortho}-1**	S112A	90 (*R*)	95
2	**biot-4^{ortho}-1**	S112A[a]	93 (*R*)	20
3	**biot-4^{ortho}-1**	S112A[b]	95 (*R*)	90
4	**biot-4^{ortho}-1**	S112Q	31 (*S*)	96
5	**biot-(*S*)-Pro-1**	S112Y	80 (*R*)	87
6	**biot-(*R*)-Pro-1**	S112G	54 (*S*)	96
7	**biot-(*R*)-Pro-1**	S112G-V47G	82 (*S*)	92

[a] No DMB added. [b] No DMB added, reaction carried out in 45% DMSO.

Thus, cyclic, sterically constrained spacers seem to project the metal center into a steric environment which favors nucleophic attack over hydrolysis.

(ii) DMB can be substituted by dimethyl sulfoxide (DMSO) with **biot-4^{ortho}-1** to yield higher enantioselectivities and comparable activities (Table 3, entries 1−3).

(iii) Whereas several ligand−protein combinations yielded good (*R*)-selectivities, achieving moderate (*S*)-selectivities proved challenging. Combining a close lying (S112G) with a more distant mutation (V47G) in combination with **biot-(*R*)-Pro-1** was required to obtain 82% ee (*S*) (Table 3, entries 6, 7).

(iv) In contrast to other reactions implemented with artificial metalloenzymes, the AAA has no equivalent in enzymatic catalysis.

The Meerwein−Pondorf−Verley Reduction and Oppenauer Oxidation

Noyori and co-workers introduced three legged pianostool complexes $[(\eta^n\text{-}C_nR_n)M(L\text{^}L')H]^{m+}$ for the asymmetric transfer hydrogenation (ATH) of prochiral aryl ketones in the presence of hydrogen donors (isopropanol or formate) (Figure 4).[21] Again here, it appears that the enantioselection proceeds without coordination of the substrate to the metal.[22] The same complexes were subsequently shown to catalyze the microscopic reverse kinetic resolution of racemic aryl alcohols.[23]

Inspired by the popular enantiopure Tos-DPEN (*p*-tolylsulfonamido-diphenyl-ethylenediamine), we synthesized d^6-pianostool complexes bearing achiral biotinylated *N*-arylsulfonamide-1,2-ethylenediamine (**biot-*q*-L**H, *q* = *ortho*, *meta*, *para*). The ligands were complexed to either $[Cp^*IrCl]^+$, $[Cp^*RhCl]^+$, or $[(\eta^6\text{-arene})RuCl]^+$, to afford 20 biotinylated complexes. These were combined with the saturation mutagenesis library S112X as well several single and double point mutants (Figure 6).[24] Instead of screening the whole chemogenetic diversity matrix, we adopted a strategy whereby all catalyst precursors were screened with a subset of Sav isoforms. Only the best biotinylated catalysts were then screened with all the proteins. The best catalyst⊂protein combinations were evaluated toward various substrates. Selected results are summarized in Table 4.

Noteworthy features for artificial transfer hydrogenases included:

(i) Artificial metalloenzymes bearing the *para*-substituted ligand **biot-*p*-L** outperformed both the **biot-*o*-L** and **biot-*m*-L** systems. Similarly, the ruthenium complexes generally yielded better activities and selectivities than either rhodium or iridium complexes.

(ii) The capping arene played a significant role in determining the enantioselectivity: $[(\eta^6\text{-benzene})Ru(\textbf{biot-}\textit{p}\textbf{-L})Cl]^+$ and $[(\eta^6\text{-}p\text{-cymene})Ru(\textbf{biot-}\textit{p}\textbf{-L})Cl]^+$ tended to produce

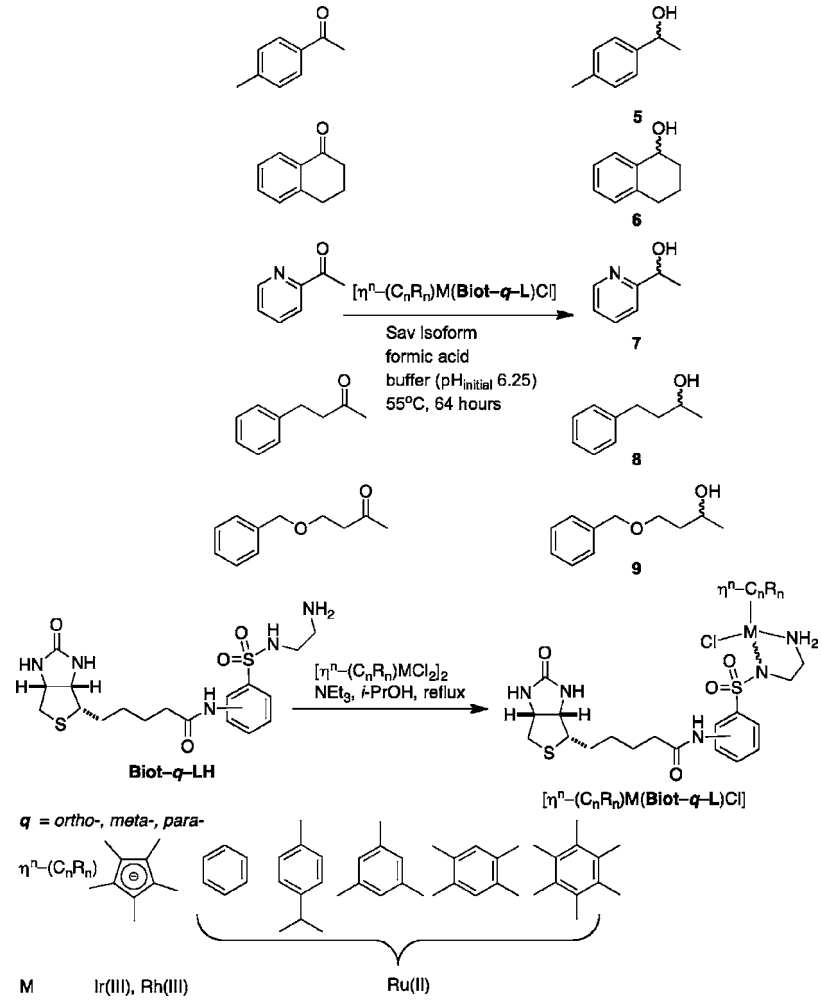

FIGURE 6. Substrates, ligands, and operating conditions for the ATH catalyzed by artificial metalloenzymes based on the biotin−avidin technology.

opposite enantiomers. This trend was most pronounced when complexes were combined with either S112K ((*S*)-selective) or S112A or S112F ((*R*)-selective).

(iii) Good enantioselectivities (ee > 90%, Table 4, entries 1−12) were obtained for arylalcohols **5**−**7**. Dialkylketones afforded only modest enantioselectivities, Table 4, entries 13, 14). We hypothesize that the enantioselection proceeds via a CH−π interaction between the η^6-arene and the substrate (Figure 4).[25] In the presence of positively charged residues at position S112, this interaction may be overruled by cation−π interaction leading to opposite enantiomers (Table 3, entries 3−6 and 11,12).

(iv) Potentially coordinating amino acids at position S112 (e.g., S112C, S112M, S112H, S112D, and S112E) strongly inhibit catalysis. This suggests that the metal center with $[(\eta^n\text{-}C_nR_n)M(\textbf{biot-}\textit{p}\textbf{-L})]^{n+}$ may interact with these residues thus preventing turnover.

TABLE 4. Numerical Summary of Selected ATH Results[a]

entry	protein	complex	product	ee (%)	conv. (%)
1	WT Sav	[η^6-(*p*-cymene)Ru(**biot-*p*-L**)Cl]	**5**	89 (*R*)	95
2	WT Sav	[η^6-(benzene)Ru(**biot-*p*-L**)Cl]	**5**	29 (*R*)	38
3	S112A	[η^6-(*p*-cymene)Ru(**biot-*p*-L**)Cl]	**5**	91 (*R*)	98
4	S112A	[η^6-(benzene)Ru(**biot-*p*-L**)Cl]	**5**	41 (*R*)	74
5	S112K	[η^6-(*p*-cymene)Ru(**biot-*p*-L**)Cl]	**5**	10 (*S*)	34
6	S112K	[η^6-(benzene)Ru(**biot-*p*-L**)Cl]	**5**	63 (*S*)	24
7	P64G	[η^6-(*p*-cymene)Ru(**biot-*p*-L**)Cl]	**5**	94 (*R*)	92
8	P64G	[η^6-(benzene)Ru(**biot-*p*-L**)Cl]	**5**	44 (*S*)	44
9	S112Y	[η^6-(*p*-cymene)Ru(**biot-*p*-L**)Cl]	**6**	97 (*R*)	79
10	S112A	[η^6-(benzene)Ru(**biot-*p*-L**)Cl]	**6**	51 (*S*)	44
11	S112R	[η^6-(benzene)Ru(**biot-*p*-L**)Cl]	**7**	70 (*S*)	95
12	S112F	[η^6-(*p*-cymene)Ru(**biot-*p*-L**)Cl]	**7**	76 (*R*)	95
13	S112A	[η^6-(*p*-cymene)Ru(**biot-*p*-L**)Cl]	**8**	48 (*R*)	98
14	S112A	[η^6-(*p*-cymene)Ru(**biot-*p*-L**)Cl]	**9**	69 (*R*)	97
15	L124 V	[η^6-(*p*-cymene)Ru(**biot-*p*-L**)Cl]	**5**	96 (*R*)	97
16	L124 V	[η^6-(*p*-cymene)Ru(**biot-*p*-L**)Cl]	**6**	87 (*R*)	20
17	S112A K121N	[η^6-(benzene)Ru(**biot-*p*-L**)Cl]	**6**	92 (*S*)	54
18	S112A K121N	[η^6-(benzene)Ru(**biot-*p*-L**)Cl]	**7**	92 (*S*)	quant.
19	S112A K121T	[η^6-(*p*-cymene)Ru(**biot-*p*-L**)Cl]	**8**	88 (*R*)	quant.
20	S112A K121W	[η^6-(benzene)Ru(**biot-*p*-L**)Cl]	**8**	84 (*R*)	quant.
21	S112A K121T	[η^6-(*p*-cymene)Ru(**biot-*p*-L**)Cl]	**9**	90 (*R*)	quant.

[a] The catalytic runs were performed at 55 °C for 64 h using the mixed buffer HCO_2Na (0.48 M) + $B(OH)_3$ (0.41 M) + MOPS (0.16 M) at $pH_{initial}$ = 6.25. Ru/substrates/formate ratio 1:100:4000 (i.e., 100 equiv substrate vs Ru).

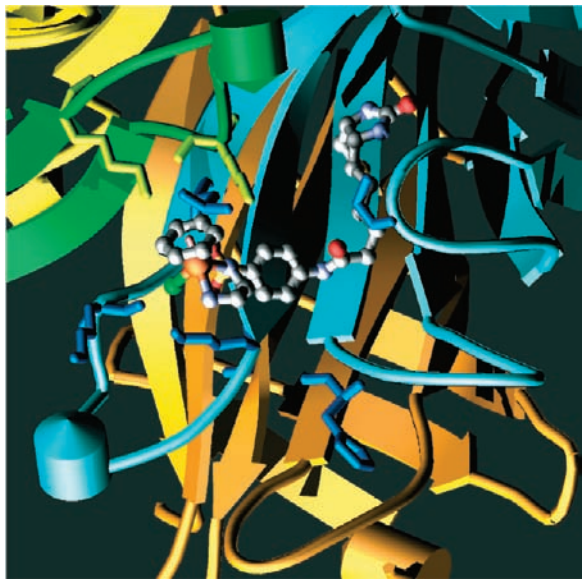

FIGURE 7. X-ray structure of an (*S*)-selective artificial ATH. Close-lying residues ($K112_A$, $L124_A$, $H87_A$, $G48_A$ $K112_B$, $K121_B$, and $K112_B$) are highlighted as sticks. Only (*S*)-[(η^6-*p*-cymene)Ru(**biot-*p*-L**)Cl] localized in monomer A (blue) is displayed (monomer B, green; monomer C and D, orange and yellow).

In collaboration with Stenkamp et al., we solved the X-ray structure of (*S*)-selective transfer-hydrogenase: [η^6-(benzene)Ru(**biot-*p*-L**)Cl]⊂S112K (Figure 7).[26] Notable features include:

(i) For a Ru-catalyst bound to the A monomer (blue cartoon representation in Figure 7), residues $K112_A$, $L124_A$, $K112_B$, and $K121_B$ are closest lying. Residue $K112_B$ is ideally positionned to interact with an incoming prochiral substrate. These observations consolidated our initial choice to produce the S112X saturation mutagenesis library.

(ii) The Ru-center is enantiopure: (*S*)-[η^6-(benzene)Ru(**biot-*p*-L**)Cl]. In homogeneous systems, this configuration leads to (*S*)-reduction products.[25] This suggests that the enantioselection mechanism for artificial transfer hydrogenases may proceed via the same mechanism (Figure 4b). It should be emphasized however that the occupancy of the biotinylated complex is only 20% in the structure. It thus remains to be demonstrated whether this is the actual position and configuration of the active catalyst.

(iii) The $Ru_A \cdots Ru_B$ distance is only 4.44 Å, suggesting that Ru_B cannot be localized in that position if a Ru_A moiety is localized in the symmetry related position. In this context, it is interesting to note that the enantioselectivity is not significantly influenced upon varying the number of equivalents (one to four) of [η^6-(arene)Ru(**biot-*p*-L**)Cl] versus the tetrameric Sav.

(iv) Substitution by a bulkier η^6-*p*-cymene leads to significant clashes with amino acid residues. This suggests that [(η^6-*p*-cymene)Ru(**biot-*p*-L**)Cl] must occupy a different position within the host protein and thus may explain the difference in enantioselectivity.

(v) Incorporation of the biotinylated complex does not lead to a significant reorganization of the host protein (rms 0.276 Å for all C_α).

Guided by this structural insight, we produced saturation mutagenesis libraries at position K121X or L124X. Limited by the need to screen using purified proteins, we focused on the following libraries: K121X, L124X, S112A-K121X, S112K-K121X, S112A-L124X, and S112K-L124X. These 120 Sav isoforms were combined with [(η^6-*p*-cymene)Ru(**biot-*p*-L**)Cl] and [(η^6-benzene)Ru(**biot-*p*-L**)Cl] and screened for the reduction of the model prochiral substrates to afford the enantioenriched alcohols **5**−**9** (Figure 6). To speed up the screening, we adapted the biotin-sepharose immobilization scheme developed for the artificial hydrogenase to immobilize crude cell extracts: following a 250 mL baffled-flask *E. coli* culture, the suspension was centrifugated, and the pellet was frozen and resuspended. After centrifugation, the supernatant was treated with biotin-sepharose. Having an excess of biotin binding sites versus the biotin-sepharose ensured that free biotin binding sites remained upon immobilization. The biotinylated catalyst was added to the immobilized protein. The excess metal complex was washed off before screening. The most promising immobilized artificial metalloenzymes were subsequently tested with purified proteins (Table 4).

Based on this protocol, which combines structural insight with both chemical and genetic optimization, significantly improved enantioselectivities were obtained both for aryl ketones (up to 97% (*R*) and 92% (*S*)) and dialkylketones (up to 90% (*R*), Table 4, entries 15−18 and 19−21, respectively). In the context of ATH, the latter substrates are challenging as the CH−π interaction cannot operate in the transition state,[27] suggesting that the protein has a significant influence on enantioselection.

In contrast to classical enantioselective catalysis starting from a prochiral substrate, high throughput assays for kinetic resolutions are more abundant and straightforward to implement.[28] Our efforts to achieve the microscopic reverse reaction (i.e., Oppenauer oxidation) for the kinetic resolution of racemic alcohols in the presence of sacrificial H_2 acceptors was met with limited success.[29] Indeed, although [η^6-(*p*-cymene)Ru(tos-DPEN)]$^+$ complexes catalyze the β-H abstraction of alcohols in acetone,[23] these reactions fail to proceed in water, even in the presence of more potent H_2 acceptors. After testing hexafluoroacetone, quinones, dioxygen, and hydrogen peroxide, we identified *tert*-butylhydroperoxide (THBP) as a suitable oxidant. The best biotinylated catalyst [(η^6-ben-

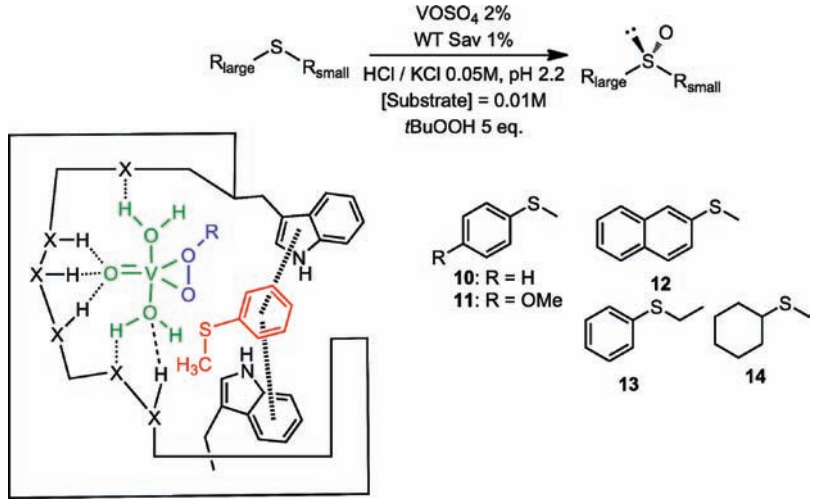

FIGURE 8. Artificial peroxidase for enantioselective sulfoxidation based on vanadyl-loaded streptavidin.

zene)Ru(**biot-*p*-L**)Cl]⊂Sav displayed >200 turnovers at room temperature. Unfortunately, no enantioenrichment of the *sec*-phenetylalcohol was observed.[29] In the absence of protein, rapid appearance of a black suspension was accompanied with much lower conversions.

Subsequently, several groups reported on their efforts to exploit dioxygen or peroxides as H_2 acceptors for the oxidation of alcohols catalyzed by d^6-pianostool complexes.[30] Most interestingly, Ikariya et al. presented a [Cp*Ir]-based oxidation catalyst which was efficient under biphasic conditions.[31]

For the oxidation of prochiral sulfides, we investigated vanadyl-based systems.

TABLE 5. Summary of Selected Sulfoxidation Results[a]

entry	protein	product	ee (%)	conv. (%)
1	WT Sav[b]	**10**	4 (*R*)	7
2		**10**	0	55
3	WT Sav	**10**	46 (*R*)	94
4	WT Sav	**11**	90 (*R*)	quant.
5	WT Sav[c]	**11**	0	96
6	D128A Sav	**11**	0	97
7	WT Sav	**12**	93 (*R*)	53
8	WT Sav	**13**	90 (*R*)	96
9	WT Sav	**14**	86 (*R*)	61
10	aviloop[d]	**14**	90 (*R*)	54

[a] All catalytic runs were performed at room temperature in 0.05 M KCl/HCl buffer at pH 2.2, with 0.0001 M WT Sav, 0.0002 M vanadium, 0.01 M sulfide, and 0.05 M *t*-BuOOH. [b] No metal added. [c] 4 equiv biotin added. [d] See ref 33.

Vanadyl-Loaded Streptavidin as Artificial Sulfoxidase

Our initial attempts to create hybrid catalysts for the oxidation of prochiral sulfides were based on [M(biot-Schiff base)]-moieties. Both conversions and selectivities remained modest.[32a] Inspired by the reports of Sheldon and co-workers on vanadyl-loaded phytase as artificial sulfoxidase,[32b] we hypothesized that the biotin-binding site of Sav may be large enough to accommodate small M═O containing coordination compounds. Various metal sources were combined with (strept)avidin and screened for their sulfoxidation properties. Vanadyl salts proved most active and selective (Figure 8 and Table 5).

(i) In the presence of THBP, $[VO(H_2O)_5]^{2+}$⊂Sav displayed increased activity (and selectivity) compared to the protein-free salt.

(ii) When biotin was added to $[VO(H_2O)_5]^{2+}$⊂Sav, racemic sulfoxide was produced. Similarly, the D128A mutant, known for its significantly reduced affinity for biotin, afforded racemic product. These data suggest that the metal moiety occupies the biotin-binding site and that the Asp128 residue is critical for the localization of the vanadyl moiety within the biotin binding site (Table 5, entries 5, 6).

(iii) Using 2 mol % $[VO(H_2O)_5]^{2+}$combined with 1 mol % tetrameric Sav at pH 2.2, a variety of aryl-alkylsulfides were oxidized in moderate to good enantioselectivities (Table 5, entries 1–8). Substitution of the short L3,4 Sav loop by the longer L3,4 loop of avidin yielded the aviloop Sav.[33] This chimeric protein improved the selectivity for dialkylsulfoxide **14** (Table 5, entries 9, 10).

(iv) X-band EPR analysis at pH 2.2 revealed an intact $[VO(H_2O)_5]^{2+}$, implying only second coordination sphere contacts between Sav and the metal.

In addition to catalyzing a myriad of small molecule transformations, enzymes reveal exquisite selectivities toward macromolecules thanks to their extended contacts with their targets. In this respect, they outperform the selectivity displayed by small molecules toward either proteins or DNA. In 1999, Crabtree et al. introduced the concept of protein display to improve the binding properties of small molecules

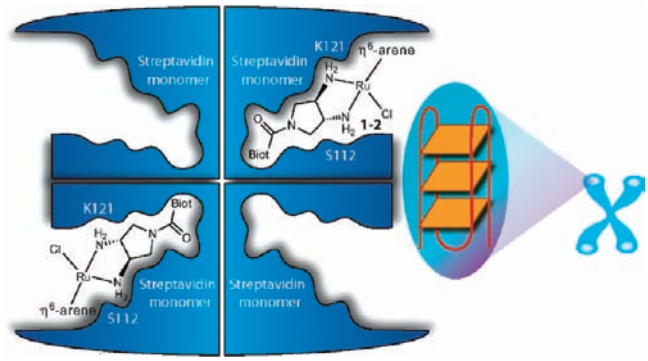

FIGURE 9. Protein display strategy applied to DNA-binding metallodrugs $[\eta^6$-(arene)Ru(**biot-en**)Cl$]^+$, arene = *p*-cymene, biphenyl.

toward a target protein or RNA.[34] We hypothesized that such an approach could be adapted to biotinylated metallodrugs to improve their selectivity toward DNA.

The Presenter-Protein Strategy

Ever since the discovery of cisplatin as a potent anticancer drug, metallodrugs have attracted much interest.[35] It is believed that the preferred target for these metals is DNA. Their poor specificity however often requires high doses, leading to undesirable side effects. With the hope of alleviating these, we hypothesized that introduction of a biotinylated d^6-pianostool complex $[\eta^6$-(arene)Ru(**biot-en**)Cl$]^+$, derived from a known metallodrug,[36] in Sav may modulate its DNA-recognition properties by providing multivalent binding interactions with the DNA target, working in concert with with metallodrug (Figure 9).

The complexes $[\eta^6$-(arene)Ru(**biot-en**)Cl$]^+$ were combined with various Sav isoforms. The X-ray structure of $[\eta^6$-(arene)Ru((*R,R*)-**biot-en**)Cl$]^+\subset$WT Sav reveals that both $K121_A$ and $K121_B$ are ideally positioned in a shallow vestibule to interact with negatively charged DNA (Figure 10). The hybrid metallodrugs were tested in vitro for their DNA affinity by electrophoretic mobility shift assays (EMSA). Selected affinities were confirmed by isothermal titration calorimetry (ITC).[37] The following trends emerged (Table 6):

(i) Neither Sav nor the biotinylated complexes $[\eta^6$-(arene)Ru(**biot-en**)Cl$]^+$ displayed high affinities toward double stranded-DNA (ds-DNA) or telomeric-DNA (tel-DNA).

(ii) The ternary complex $[(\eta^6$-*p*-cymene)Ru(**biot-en**)Cl$]\subset$ Sav·DNA was more stable (at least an order of magnitude) than Sav·DNA.

(iii) tel-DNA was recognized preferentially over ds-DNA. We speculate that the rigidity of the double-strand prevented its interaction with the host protein.

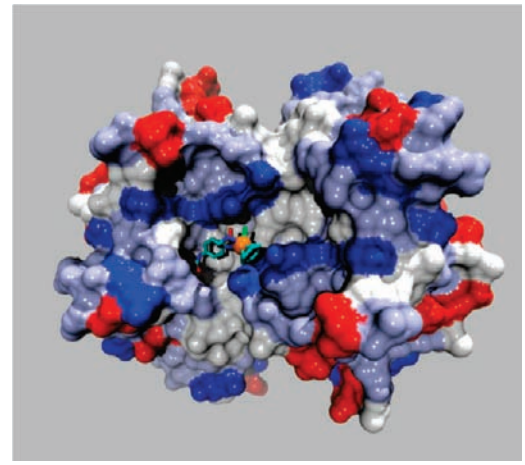

FIGURE 10. View of the X-ray structure of $[\eta^6$-(*p*-cymene)Ru((*R,R*)-**biot-en**)Cl$]^+\subset$WT Sav. Only one biotinylated complex is displayed for clarity.

TABLE 6. Summary of Dissociation Constants for Ruthenium–Streptavidin (Sav) Assemblies toward Various DNA Targets, Estimated by EMSA

entry	DNA target	complex	Sav	K_d (μM)
1	tel-DNA[a]		WT	>145
2	tel-DNA[a]	$[\eta^6$-(*p*-cymene)Ru(**biot-en**)Cl$]^+$	WT	<1.6[c]
3	tel-DNA[a]	$[\eta^6$-(*p*-cymene)Ru(**biot-en**)Cl$]^+$	S112F	<1.6[c]
4	tel-DNA[a]	$[\eta^6$-(*p*-cymene)Ru(**biot-en**)Cl$]^+$	S112D	12.2
5	tel-DNA[a]	$[\eta^6$-(*p*-cymene)Ru(**biot-en**)Cl$]^+$	K121A	28
6	tel-DNA + GSH[a,b]	$[\eta^6$-(*p*-cymene)Ru(**biot-en**)Cl$]^+$	WT	<1.6[c]
7	ds-DNA[d]	$[\eta^6$-(*p*-cymene)Ru(**biot-en**)Cl$]^+$	WT	37.9
8	ds-DNA[d]	$[\eta^6$-(*p*-cymene)Ru(**biot-en**)Cl$]^+$	S112F	37.9
9	ds-DNA[d]	$[\eta^6$-(biphenyl)Ru(**biot-en**)Cl$]^+$	WT	37.9
10	ds-DNA[d]	$[\eta^6$-(biphenyl)Ru(**biot-en**)Cl$]^+$	S112F	18.2

[a] tel-DNA; G4A sequence: catggtggtttgggttagggttagggttagggttaccac.[38] [b] In brackets, competing species: glutathione (GSH). [c] Binding was stoichiometric and beyond the sensitivity of EMSA. [d] ds-DNA; Braf oncogenic mutation V599E: ctagctacagagaaatctcga and the corresponding complementary strand.[39]

(iv) The presence of competing targets including gluthatione did not erode the affinity toward tel-DNA.

(v) Chemogenetic optimization was used to modulate the affinity of $[(\eta^6$-*p*-cymene)Ru(**biot-en**)Cl$]\subset$Sav toward its target. Charged amino acid residues in the vicinity of the metal played a critical role in determining the affinity toward negatively charged DNA: both K121A or S112D mutants displayed reduced affinity toward tel-DNA. Combining $[(\eta^6$-biphenyl)Ru(**biot-en**)Cl$]\subset$S112F increased the affinity toward ds-DNA.

Outlook

In the past years, we have focused on exploring the potential artificial metalloenzymes for various purposes. Looking back at the pros and cons of homogeneous versus enzymatic catalysis (Table 1), it appears that such hybrid systems display features reminiscent both of kingdoms. Adding precious metals to the enzymatic repertoire opens fascinating perspec-

tives. A major challenge remains: the implementation of directed evolution protocols for optimization. Thus far, all efforts to screen on colonies or culture supernatants have remained vain. Although the immobilization procedure or the "en masse" affinity purification is viable for screening small libraries, alternative strategies must be developed, including more robust organometallic catalysts, compatible with cell debris. This will allow evolution of artificial metalloenzymes for transformations which have no equivalent either in homogeneous or in enzymatic catalysis, thus rendering them more attractive for large scale applications.

Considering the versatility of homogeneous catalysis for the synthesis of enantiopure small molecules, we believe that the true potential of artificial metalloenzymes may be revealed in chemical biology applications, including in vivo catalysis for metabolic engineering, post-translational modifications of proteins, artificial restriction enzymes, and so on. Our initial effort exploiting the protein-display strategy represents a first step in this direction.

This research was supported by the Swiss National Science Foundation (Grants FN 200020-113348 and 200020-126366), the Cantons of Basel, as well as Marie Curie Training Networks IBAAC and BIOTRAINS (FP6-MRTN-CT-2003-505020 and FP7-ITN-238531). T.R.W. thanks his co-workers listed in the references for their efforts and devotion. T.R.W. thanks Andy Borovik (UC Irvine) for his hospitality during the redaction of this Account.

BIOGRAPHICAL INFORMATION

Thomas R. Ward received his PhD from ETH Zürich (with L. M. Venanzi, 1991). After two postdocs (with R. Hoffmann, Cornell Univ. and C. Floriani, Univ. Lausanne), he started his career at the University of Berne in 1993 as a Werner fellow. He was professor at the University of Neuchâtel (2000–2008) before joining the University of Basel.

FOOTNOTES

*E-mail: thomas.ward@unibas.ch.

REFERENCES

1 Jacobsen, E. N., Pfaltz, A., Yamamoto, H., Eds. *Comprehensive Asymmetric Catalysis*; Springer: Berlin, 1999.

2 Breuer, M.; Ditrich, K.; Habicher, T.; Hauer, B.; Kesseler, M.; Stürmer, R.; Zelinski, T. Industrial methods for the production of optically active intermediates. *Angew. Chem., Int. Ed.* **2004**, *43*, 788–824.

3 Taylor, S. V.; Kast, P.; Hilvert, D. Investigating and engineering enzymes by genetic selection. *Angew. Chem., Int. Ed.* **2001**, *40*, 3310–3335.

4 Berkessel, R.; Gröger, H. *Asymmetric Organocatalysis: From Biomimetic Concepts to Applications in Asymmetric Synthesis*; Wiley-VCH: Weinheim, 2005.

5 Ward, T. R., Ed. *Bio-Inspired Catalysts*; Springer: New York, 2009; Vol. 25.

6 (a) Yamamura, K.; Kaiser, E. T. Studies on the oxidase activity of Copper(II) carboxypeptidase. *J. Chem. Soc., Chem. Commun.* **1976**, 830–831. (b) Levine, H. L.; Nakagawa, Y.; Kaiser, E. T. Flavopapain: synthesis and properties of semisynthetic enzymes. *Biochem. Biophys. Res. Commun.* **1977**, *76*, 64–71.

7 Wilson, M. E.; Whitesides, G. M. Conversion of a protein to a homogeneous asymmetric hydrogenation catalyst by site specific modification with a diphosphinerhodium(I) moiety. *J. Am. Chem. Soc.* **1978**, *100*, 306–307.

8 (a) Wu, Z.-P.; Hilvert, D. Conversion of a protease into an acyl transferase: selenosubtilisin. *J. Am. Chem. Soc.* **1989**, *111*, 4513–4514. (b) Roy, R. S.; Imperiali, B. Pyridoxamine-amino acid chimeras in semisynthetic aminotransferase mimics. *Protein Eng.* **1997**, *10*, 691–698. (c) Lin, C.-C.; Lin, C.-W.; Chan, A. S. C. Catalytic hydrogenation of itaconic acid in a biotinylated pyrphos-rhodium(I) system in a protein cavity. *Tetrahedron: Asymmetry* **1999**, *10*, 1887–1893. (d) Qi, D.; Tann, C.-M.; Haring, D.; Distefano, M. D. Generation of new enzymes via covalent modification of existing proteins. *Chem. Rev.* **2001**, *101*, 3081–3111.

9 (a) Yamaguchi, H.; Hirano, T.; Kiminami, H.; Taura, D.; Harada, A. Asymmetric hydrogenation with antibody-achiral rhodium complex. *Org. Biomol. Chem.* **2006**, *4*, 3571–3573. (b) Lu, Y.; Yeung, N.; Sieracki, N.; Marshall, N. M. Design of functional metalloproteins. *Nature* **2009**, *460*, 855–862. (c) Reetz, M. T. Directed Evolution of Stereoselective Hybrid Catalysts. *Top. Organomet. Chem.* **2009**, *25*, 63–92. (d) Jing, Q.; Okrasa, K.; Kazlauskas, R. J. Stereoselective hydrogenation of olefins using rhodium-substituted carbonic anhydrase - A new reductase. *Chem.—Eur. J.* **2009**, *15*, 1370–1376. (e) Abe, S.; Ueno, T.; Watanabe, Y. Artificial metalloproteins exploiting vacant space: preparation, structures, and functions. *Top. Organomet. Chem.* **2009**, *25*, 25–43. (f) Boersma, A. J.; Megens, R. P.; Feringa, B. L.; Roelfes, G. DNA-based asymmetric catalysis. *Chem. Soc. Rev.* **2010**, *39*, 2083–2092.

10 Duclos, S.; Ward, T. R.; Stoeckli-Evans, H. Design and synthesis of compartmental ligands and their complexes for catalytic antibodies. *Helv. Chim. Acta* **2001**, *84*, 3148–3161.

11 Humbert, N.; Zocchi, A.; Ward, T. R. Electrophoretic behavior of streptavidin complexed to a biotinylated probe: a functional screening assay for biotin-binding proteins. *Electrophoresis* **2005**, *26*, 47–52.

12 Collot, J.; Gradinaru, J.; Humbert, N.; Skander, M.; Zocchi, A.; Ward, T. R. Artificial metalloenzymes for enantioselective catalysis based on biotin-avidin. *J. Am. Chem. Soc.* **2003**, *125*, 9030–9031.

13 Mazurek, S.; Ward, T. R.; Novic, M. Counter propagation artificial neural networks modeling of an enantioselectivity of artificial metalloenzymes. *Mol. Diversity* **2007**, *11*, 141–152.

14 Klein, G.; Humbert, N.; Gradinaru, J.; Ivanova, A.; Gilardoni, F.; Rusbandi, U. E.; Ward, T. R. Tailoring the active site of chemzymes by using a chemogenetic-optimization procedure: towards substrate-specific artificial hydrogenases based on the biotin-avidin technology. *Angew. Chem., Int. Ed.* **2005**, *44*, 7764–7767.

15 Wahler, D.; Badalassi, F.; Crotti, P.; Reymond, J.-L. Enzyme fingerprints of activity, stereo and enantioselectivity from fluorogenic and chromogenic substrate arrays. *Chem.—Eur. J.* **2002**, *8*, 3211–3228.

16 Rusbandi, U. E.; Lo, C.; Skander, M.; Ivanova, A.; Creus, M.; Humbert, N.; Ward, T. R. Second generation artificial hydrogenases based on the biotin avidin technology: improving activity, stability and selectivity by introduction of enantiopure aminoacid spacers. *Adv. Synth. Catal.* **2007**, *349*, 1923–1930.

17 Reetz, M. T.; Peyeralans, J. J.-P.; Maichele, A.; Fu, Y.; Maywald, M. Directed evolution of hybrid enzymes: evolving enantioselectivity of an achiral Rh-complex anchored to a protein. *Chem. Commun.* **2006**, 4318–4320.

18 (a) Trost, B. M.; Crawley, M. L. Asymmetric transition-metal-catalyzed allylic alkylations: applications in total synthesis. *Chem. Rev.* **2003**, *103*, 2921–2943. (b) Tsuji, J. *Palladium in Organic Synthesis*; Springer: Berlin, Heidelberg and New York, 2005; Vol. 14.

19 Helmchen, G.; Pfaltz, A. Phosphinooxazolines: a new class of versatile, modular P, N-ligands for asymmetric catalysis. *Acc. Chem. Res.* **2000**, *33*, 336–345.

20 Pierron, J.; Malan, C.; Creus, M.; Gradinaru, J.; Hafner, I.; Ivanova, A.; Sardo, A.; Ward, T. R. Artificial metalloenzymes for asymmetric allylic alkylation on the basis of the biotin-avidin technology. *Angew. Chem., Int. Ed.* **2008**, *47*, 701–705.

21 (a) Noyori, R.; Hashiguchi, S. Asymmetric transfer hydrogenation catalyzed by chiral ruthenium complexes. *Acc. Chem. Res.* **1997**, *30*, 97–102. (b) Ikariya, T.; Murata, K.; Noyori, R. Bifunctional transition metal-based molecular catalysts for asymmetric syntheses. *Org Biomol Chem* **2006**, *4*, 393–406.

22 Haack, K.-J.; Hashiguchi, S.; Fujii, A.; Ikariya, T.; Noyori, R. The catalyst precursor, catalyst and intermediate in the Ru(II)-promoted asymmetric hydrogen transfer between alcohols and ketones. *Angew. Chem., Int. Ed. Engl.* **1997**, *36*, 285–288.

23 Hashiguchi, S.; Fujii, A.; Haack, K.-J.; Matsumura, K.; Ikariya, T.; Noyori, R. Kinetic resolution of racemic secondary alcohols by a Ru(II)-catalyzed hydrogen transfer. *Angew. Chem., Int. Ed. Engl.* **1997**, *36*, 288–290.

24 (a) Letondor, C.; Humbert, N.; Ward, T. R. Artificial metalloenzymes based on biotin-avidin technology for the enantioselective reduction of ketones by transfer hydrogenation. *Proc. Natl. Acad. Sci. U.S.A.* **2005**, *102*, 4683–4687. (b) Letondor, C.; Pordea, A.; Humbert, N.; Ivanova, A.; Mazurek, S.; Novic, M.; Ward, T. R. Artificial transfer hydrogenases based on the biotin-(strept)avidin technology: fine

tuning the selectivity by saturation mutagenesis of the host protein. *J. Am. Chem. Soc.* **2006**, *128*, 8320–8328.

25 Yamakawa, M.; Yamada, I.; Noyori, R. CH/π attraction; the origin of enantioselectivity in transfer hydrogenation of aromatic carbonyl compounds catalyzed by chiral η^6-arene ruthenium(II) complexes. *Angew. Chem., Int. Ed.* **2001**, *40*, 2818–2821.

26 Creus, M.; Pordea, A.; Rossel, T.; Sardo, A.; Letondor, C.; Ivanova, A.; LeTrong, I.; Stenkamp, R. E.; Ward, T. R. X-Ray structure and designed evolution of an artificial transfer hydrogenase. *Angew. Chem., Int. Ed.* **2008**, *47*, 1400–1407.

27 Schlatter, A.; Woggon, W.-D. Enantioselective transfer hydrogenation of aliphatic ketones catalyzed by ruthenium complexes linked to the secondary face of beta-cyclodextrin. *Adv. Synth. Catal.* **2008**, *350*, 995–1000.

28 (a) Reetz, M. T. New methods for the high-throughput screening of enantioselective catalysts and biocatalysts. *Angew. Chem., Int. Ed.* **2002**, *41*, 1335–1338. (b) Finn, M. G. Emerging methods for the rapid determination of enantiomeric excess. *Chirality* **2002**, *14*, 534–540. (c) Reymond, J.-L.; Fluxa, V. S.; Maillard, N. Enzyme Assays. *Chem. Commun.* **2009**, 34–36.

29 Thomas, C. M.; Letondor, C.; Humbert, N.; Ward, T. R. Aqueous oxidation of alcohols catalyzed by artificial metalloenzymes based on the biotin-avidin technology. *J. Organomet. Chem.* **2005**, *690*, 4488–4491.

30 Heiden, Z.; Rauchfuss, T. Homogeneous catalytic reduction of dioxygen using transfer hydrogenation catalysts. *J. Am. Chem. Soc.* **2007**, *129*, 14303–14310.

31 Arita, S.; Koike, T.; Kayaki, Y.; Ikariya, T. Aerobic oxidative kinetic resolution of racemic secondary alcohols with chiral bifunctional amido complexes. *Angew. Chem., Int. Ed.* **2008**, *47*, 2447–2449.

32 (a) Pordea, A.; Mathis, D.; Ward, T. R. Incorporation of biotinylated manganese-salen complexes into streptavidin: new artificial metalloenzymes for enantioselective sulfoxidation. *J. Organomet. Chem.* **2009**, *694*, 930–936. (b) van de Velde, F.; Könemann, L.; Rantwijk, F. v.; Sheldon, R. A. Enantioselective sulfoxidation mediated by vanadium-incorporated phytase: a hydrolase acting as a peroxidase. *Chem. Commun.* **1998**, 1891–1892.

33 Eisenberg-Domovich, Y.; Pazy, Y.; Nir, O.; Raboy, B.; Bayer, E. A.; Wilchek, M.; Livnah, O. Structural elements responsible for conversion of streptavidin to a pseudoenzyme. *Proc. Natl. Acad. Sci. U.S.A.* **2004**, *101*, 5916–5921.

34 (a) Briesewitz, R.; Ray, G.; Wandless, T.; Crabtree, G. Affinity modulation of small-molecule ligands by borrowing endogenous protein surfaces. *Proc. Natl. Acad. Sci. U.S.A.* **1999**, *96*, 1953–1958. (b) Harvey, I.; Garneau, P.; Pelletier, J. Forced engagement of a RNA/protein complex by a chemical inducer of dimerization to modulate gene expression. *Proc. Natl. Acad. Sci. U.S.A.* **2002**, *99*, 1882–1887.

35 (a) Yan, Y. K.; Melchart, M.; Habtemariam, A.; Sadler, P. J. Organometallic chemistry, biology and medicine: ruthenium arene anticancer complexes. *Chem. Commun.* **2005**, 4764–4776. (b) Jung, A.; Lippard, S. J. Direct cellular response to platinum-induced DNA damage. *Chem. Rev.* **2007**, *107*, 1387–1407.

36 Bruijnincx, P. C. A.; Sadler, P. J. New Trends for metal complexes with anticancer activity. *Curr. Opin. Chem. Biol.* **2008**, *12*, 197–206.

37 Zimbron, M. J.; Sardo, A.; Heinisch, T.; Wohlschlager, T.; Gradinaru, J.; Massa, C.; Schirmer, T.; Creus, M.; Ward, T. R. Chemo-genetic optimization of DNA recognition by metallodrugs using a presenter protein strategy. *Chem.—Eur. J.* **2010**, in press.

38 Han, F. X.; Wheelhouse, R. T.; Hurley, L. H. Structural basis for the differential effects on telomerase inhibition. *J. Am. Chem. Soc.* **1999**, *121*, 3561–3569.

39 Namba, H.; Nakashima, M.; Hayashi, T.; Hayashida, N.; Maeda, S.; Rogounovitch, T. I.; Ohtsuru, A.; Saenko, V. A.; Kanematsu, T.; Yamashita, S. Clinical implication of hot spot BRAF mutation, V599E, in papillary thyroid cancers. *J. Clin. Endocrinol. Metab.* **2003**, *88*, 4393–4397.